Unsteady transonic flow behind an axisymmetric afterbody with two boosters

P. Meliga[1] and P. Reijasse[2]
ONERA, Fundamental and Experimental Aerodynamics Department
8 rue des Vertugadins, 92190 Meudon, France

The transonic flow past a three-dimensional afterbody is investigated experimentally through wall-pressure measurements. We use a three-body geometry representative of a realistic launcher afterbody, made of an axisymmetric main body equipped with a propulsive nozzle, with two removable cylindrical boosters mounted at diametrically opposed positions. We observe that the presence of the boosters alters significantly the flow dynamics. The three-body separated area is dissymmetric and is characterized by a massive pressure drop and high levels of fluctuations. The unsteady features of the flow are also modified, namely the frequency and azimuthal wavenumber selection in the separation switches from the m=1 mode at the Strouhal number St~0.2 in the axisymmetric case to a m=0 mode at the Strouhal number St~0.34 in the three-dimensional case. This contrasts with the effects reported by other authors, which involves more complex afterbodies and nozzle profiles.

Nomenclature

∞	=	relative to the upstream flow quantities
D	=	afterbody diameter
L	=	rear-body length
St_l	=	Strouhal number based from the length scale l
p	=	static pressure
p'	=	pressure fluctuation
C_P	=	pressure coefficient
C_{Prms}	=	pressure fluctuations coefficient
S_{xx},S_{xy}	=	auto-correlation and cross-correlation functions

I. Introduction

LAUNCHER afterbody flows are characterized by a massive separation occurring at the base region due to an abrupt change in the rear geometry. The unsteadiness of the separated flow generates strong low frequency wall-pressure fluctuations and induces aerodynamic excitation. The resulting high dynamic loads can trigger a response of the structural modes, termed buffeting, that can be critical during the transonic phase of flight, as experienced by the Ariane V launcher.

The properties of the base pressure of separated flows have been experimentally and theoretically studied in the last decades[6,8,11]. For complex afterbody shapes[1,2,4,10], several aerodynamics phenomena are simultaneously at work (recirculating area, reattachment of the separated shear layer on a solid surface, acoustic radiation of the propulsive jet), and limit the knowledge of the separated dynamics. Reducing the pressure fluctuations level in order to improve the performances and the reliability of the future launch vehicles hence remains a challenge.

A study by Deprés et al.[3,5] has enlightened the wall-pressure properties of axisymmetric blunt configurations equipped with a cylindrical rear-body of variable length. The main idea developed in this study is that despite the broad variety of control parameters, two main kinds of separation are to be considered, depending on whether the

[1]PhD student, ONERA/Fundamental and Experimental Aerodynamics Department, meliga@onera.fr
[2]Research Engineer, ONERA/Fundamental and Experimental Aerodynamics Department.

separated external flow does or does not reattach on the rear-body. For short rear-bodies, the flow organisation is dominated by the periodic shedding of large scale vortical structures, as observed for bluff bodies, as shown by the far wake velocity measurements of Flodrops and Desse[7]. For sufficiently long rear-bodies, the unsteady dynamics is dominated by the reattachment process of the separated shear layer (see the review of Mabey[9]). The high intensity fluctuations can then be ascribed to the shear layer vortices impinging the downstream surface.
This paper presents an experimental investigation of more realistic afterbody geometries: we use the same axisymmetric models as Deprés *et al*, equipped with two removable cylindrical boosters mounted at diametrically opposed positions. Based on wall-pressure measurements, we aim at characterizing the unsteady activity of the three-dimensional separated area.

II. Experimental Setup

Tests are carried out in the S3Ch continuous transonic wind tunnel of ONERA. The main body is made of an axisymmetric blunt-based body of diameter D = 100mm equipped with a cylindrical rear-body of diameter d=40mm, whose exit plane is located at a distance L downstream of the base (Figure 1a). The main body can be equipped at diametrically opposed positions with two cylindrical boosters of diameter D_b=65mm and length 576mm, whose extremity plane is located at a distance 77mm downstream of the main body base plane (Figure 1b). Two rear-bodies of respective lengths L=60mm (aspect ratio L/D=0.6) and L=120mm (L/D=1.2) are considered here. These aspect ratios 0.6 and 1.2 of the rear-body were chosen because they correspond, in the context of axisymmetric afterbodies, to a separated shear layer reattaching downstream of the rear-body exit plane and to a separated shear layer reattaching near the vicinity of the rear-body. Each booster is attached to the main body by the two struts device shown in Figure 1a, which is symmetrical with respect to the booster plane. Steady and unsteady wall-pressure measurements are performed using 77 pressure taps mounted on the cylindrical forebody, the base area, and the rear-body region, both in the streamwise and azimuthal directions. Time histories of the unsteady pressures are recorded over 12 seconds. The static component is measured using 12 Statham sensors, and the fluctuating component is recorded simultaneously using 65 Kulite sensors, at a sampling rate of 10240 Hz.

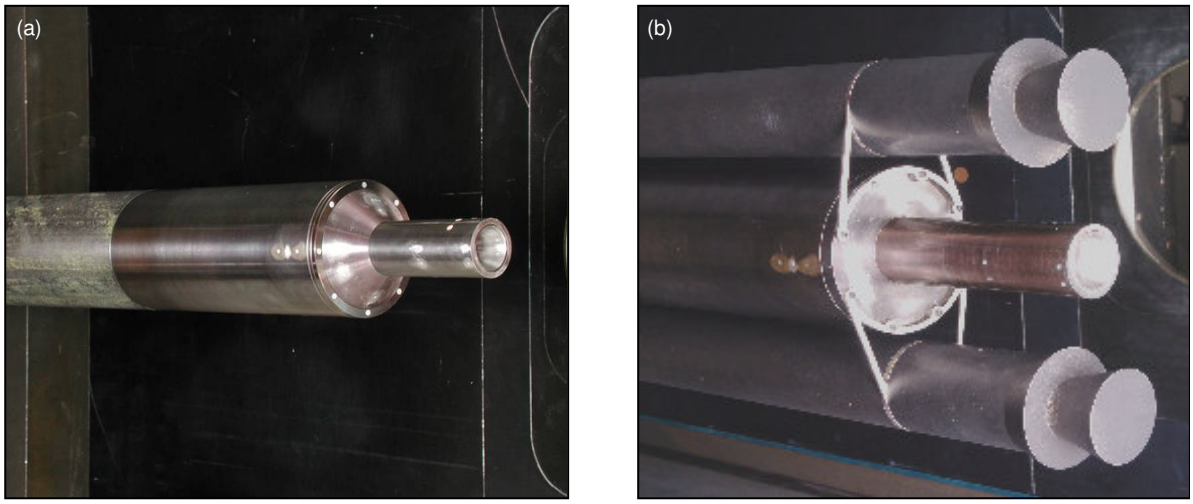

Figure 1. a) Main body of the L/D=0.6 axisymmetric model. b) L/D=1.2 three-body configuration and rear struts device (the front device is identical).

The models are mounted at the end of a cylindrical forebody fixed in the wind-tunnel settling chamber, and all tests are performed at zero incidence. The initial external boundary layer grows on the upstream cylindrical sting over a distance of over 10D before reaching the base corner. Because the setup of the Mach and Reynolds numbers could not be done independently, the Reynolds number based on the forebody diameter D varies from $1.35*10^6$ at M = 0.7 to $2.60*10^6$ at M = 0.9. The models were tested with and without boosters, for upstream conditions M_∞=0.7 and 0.9. Different internal flow regimes were then considered: no jet, jet at adaptation, and over expanded jet with separation. In this analysis, we discuss only the no jet configurations at M_∞=0.7, as no significant effect of the jet was found, due to the limited interaction between the afterbody and the jet shear layers.

III. Results

The three-body model has two planes of symmetry: in the following, the B-plane denotes the booster plane, containing the axis of revolution and the boosters, and corresponding to azimuthal positions θ=0 [π]. The no-booster plane, or NB-plane, is orthogonal to the B-plane and corresponds to azimuthal positions θ= π/2 [π], as shown in Figure 2.

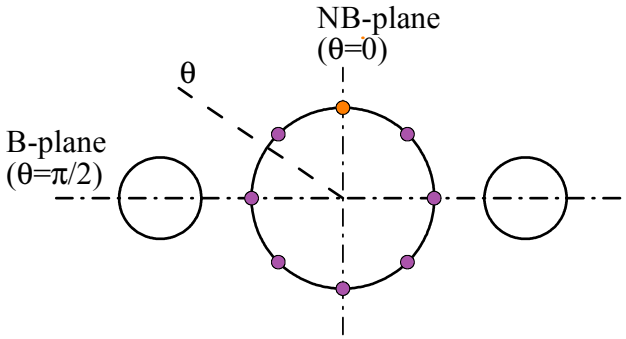

Figure 2. Geometry and location of the sensors for the two-point analysis.

In the following, we use the non-dimensional C_p and C_{prms} coefficients built from the free stream dynamic pressure q_∞, respectively defined as

$$C_P = (p - p_\infty)/q_\infty, \qquad C_{\mathrm{Pr}ms} = \sqrt{\overline{p'^2}}/q_\infty \tag{1}$$

Wall-pressure spectra are investigated along the θ=0 and θ= π/2 axis XXX, in order to estimate the three-dimensionality of the separation, and to identify the most energetic frequencies involved in the flow unsteadiness. For L/D=0.6 (resp. L/D=1.2), the Strouhal number is built from the upstream velocity and the main body diameter D (resp. the rear-body length L):

$$St_D = fD/U_\infty \qquad (L/D = 0.6) \tag{2}$$

$$St_D = fL/U_\infty \qquad (L/D = 1.2) \tag{3}$$

The pressure auto-correlation function S_{xx} is analyzed for streamwise sensor distributions located in the NB-plane. Cross-correlations are also investigated for circumferential sensor distributions located at a given streamwise position (purple points in Figure 2), the reference sensor being always located in the NB-plane, at the azimuthal position θ=0 (orange point in Figure 2). Considering the cross-correlation function S_{xy} between two sensors x and y, S_{xx} and S_{yy} being the respective auto-correlation functions, we investigate the normalized cross-correlation function C and its Fourier decomposition in azimuthal modes, defined as

$$C(St, \Delta\theta, \Delta x) = S_{xy}(St, \Delta\theta, \Delta x)/\sqrt{S_{xx}(St)S_{yy}(St)} \tag{4}$$

$$C(St, \Delta\theta, \Delta x) = \sum_m C_m(St, \Delta x)e^{im\Delta\theta} \tag{5}$$

Results are provided in terms of the coherence function $\gamma = |C|$ and of the azimuthal coherence function $\gamma_m = |C_m|$, which can be seen as the percentage of fluctuating energy relative to the m^{th} azimuthal mode at a given frequency.

A. Axisymmetric configurations

The results obtained without boosters show a very good agreement with those reported by Deprés *et al*[4,5]. As a matter of fact, for the ratio L/D=0.6, the power density spectra of the pressure fluctuations in the separated area are

dominated by a narrow peak at the Strouhal number $fD/U_\infty \sim 0.2$ corresponding to the vortex shedding phenomenon (Figure 3a). Figure 3b presents the coherence spectra for the modes of azimuthal wavenumbers $|m| < 4$ at $x/D = 0.55$, i.e. the azimuthal Fourier decomposition of the complex coherence function as a function of the frequency. The vortex shedding is due to the existence of a highly coherent mode of azimuthal wavenumber $m = 1$, whose energy represents ~ 95% of the pressure fluctuations measured at this frequency and position.

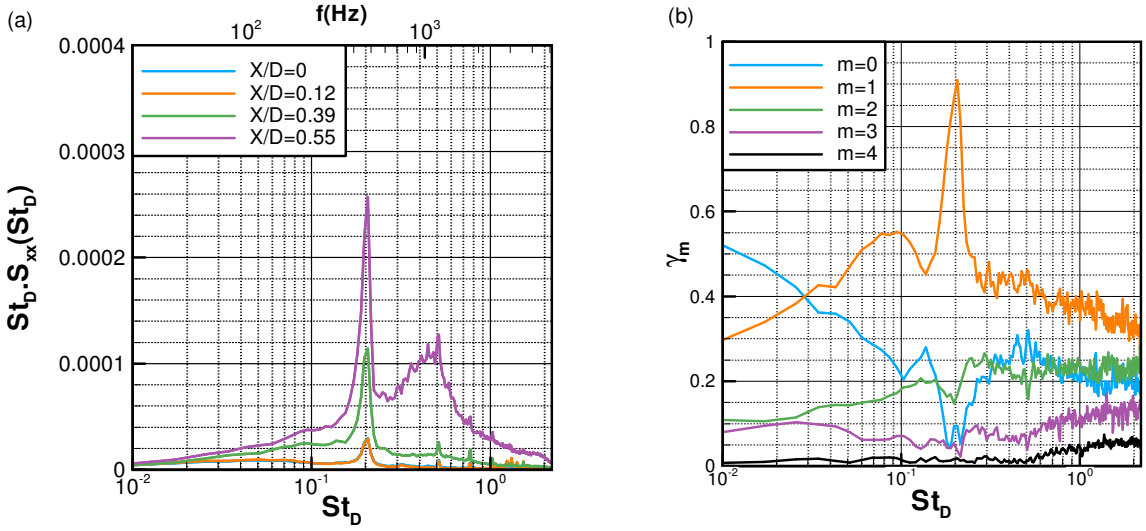

Figure 3. L/D=0.6 axisymmetric configuration. a) Pressure spectra on the rear-body. b) Coherence spectra of the first five azimuthal modes.

For the ratio L/D=1.2, a narrow peak at the Strouhal number $fL/U_\infty \sim 0.2$ is still identifiable inside the recirculation zone (x/D<1), the associated m=1 mode contributing for more than 85% in the fluctuations at this frequency for x/D=0.72 (Figure 4a and 4b). Near the end of the nozzle (x/D=0.55), the peak persists but the energy spectrum is dominated by broadband energy frequencies of magnitude three to four times larger than the vortex shedding frequency, and corresponds to shear layer vortices impinging the rear-body surface. This results in the loss of coherence of the m=1 mode observed in Figure 4b at x/D=1.15. Note that the lower level of coherence of this mode at x/D=0 is due to the low frequency flapping of the shear layer involving the axisymmetric m=0 mode.

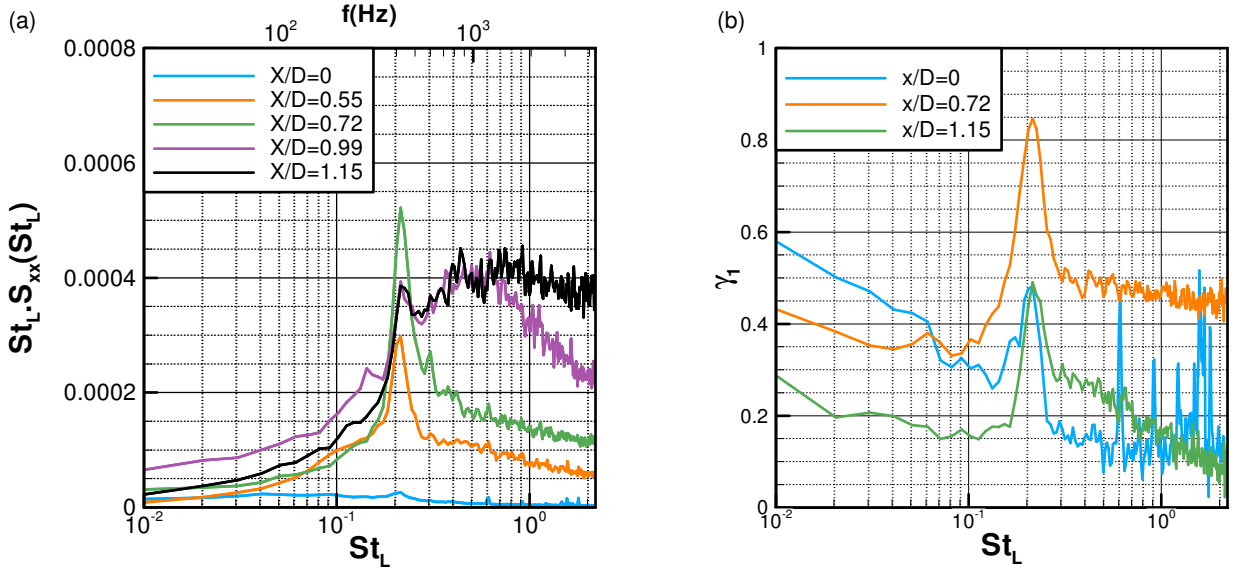

Figure 4. L/D=1.2 axisymmetric configuration. a) Pressure spectra on the rear-body. b) Coherence spectra of the first azimuthal modes for different streamwise positions.

B. Three-body configurations

In the three-body case, the difference between the two ratios L/D=0.6 and 1.2 is less clear. Figures 3 and 4 present respectively the streamwise distributions of C_P and C_{Prms} for both values of L/D. Compared to the axisymmetric case, the three-dimensional separation is characterized by a massive pressure drop and by a strong increase of the level of fluctuations, which can reach up to 7% (L=0.6) and 9% (L=1.2) of the upstream dynamic pressure (2% and 4% for the axisymmetric case). For both values of L/D, the distributions of pressure fluctuations indicate that the separated area is dissymmetric with respect to the B- and NB-planes (Figure 6). For L/D=0.6, the separated shear layer does not reattach, as the maximum of the fluctuations is obtained at the end of the rear-body, but the highest rate of growth obtained for x/D>0.4 in the NB-plane indicates that the separation may be shorter in this plane. This is confirmed by the results obtained for L/D=1.2, where the maximum of fluctuations corresponding to the reattachment of the separated shear layer is obtained for x/D~0.7 in the NB-plane and x/D~1 in the B-plane. A possible explanation for this three-dimensionality is that the incoming flow is *free* in the NB-plane, i.e. the separated shear layer behaves identically to that of an axisymmetric afterbody, and *forced* in the B-plane, i.e. the reattachment length is triggered by the separation of the boundary layer developing on the boosters, as suggested by the instantaneous schlieren photograph in Figure 7.

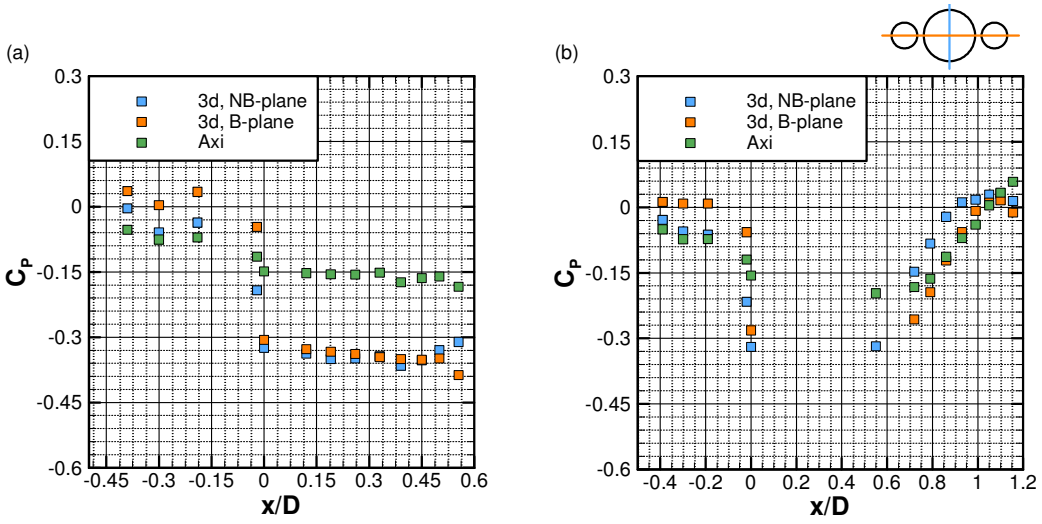

Figure 5. Streamwise evolution of the static pressure. a) L/D=0.6. b) L/D=1.2.

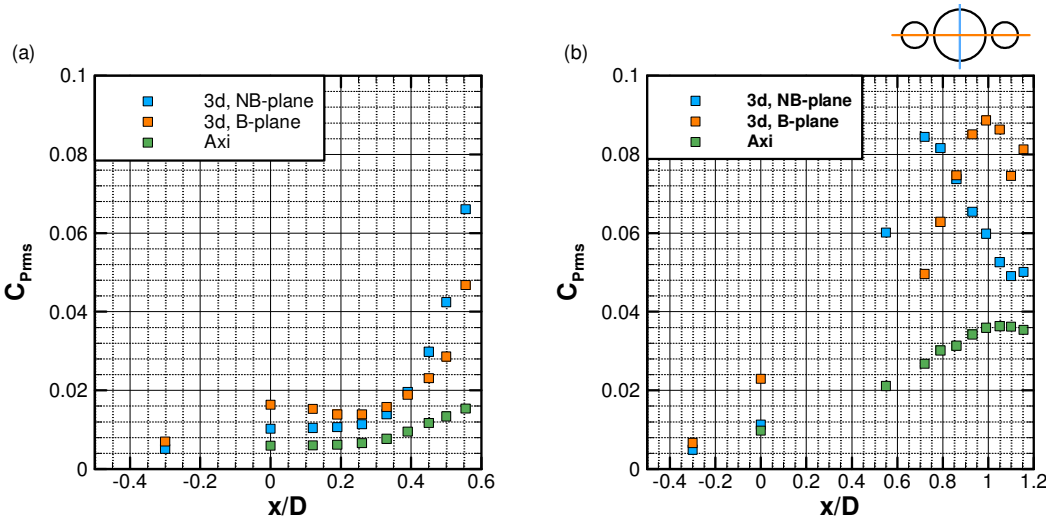

Figure 6. Streamwise evolution of the pressure fluctuations. a) L/D=0.6. b) L/D=1.2.

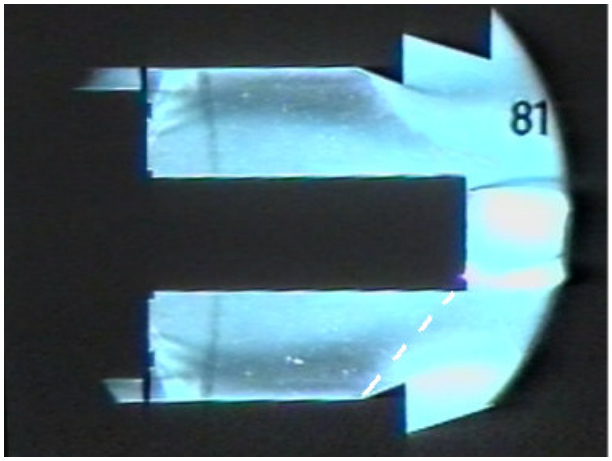

Figure 7. Schlieren photograph of the B-plane for the L/D=1.2 configuration. The dashed thick line corresponds to the external envelope of the shear layer separating from the lower booster.

For L/D=0.6, the spectral analysis show a significant change in the spatial organisation of the separated flow, as the pressure fluctuations spectra are dominated near the base by a peak at the Strouhal number $fD/U_\infty \sim 0.31$, as shown in Figure 8. Near the end of the nozzle, this peak does not appear in the NB-plane where the spectra are dominated by high frequency broadband fluctuations, a result similar to that observed for the L/D=1.2 axisymmetric case and confirming that the separation is shorter in this plane, and that the shear layer vortices partially impinge the extremity of the rear-body, although no reattachment occurs. The spectra in the B-plane show that the lower levels of fluctuations observed in this plane (Figure 5b) are due to a lower intensity of the high frequencies, consistently with the idea that the separation is larger in the B-plane.

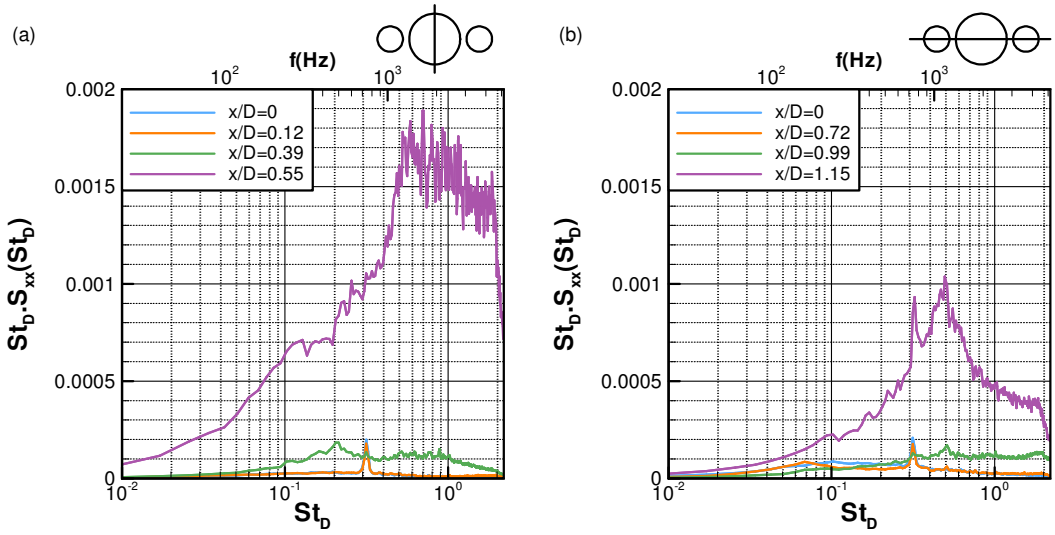

Figure 8. Spectra of the pressure fluctuations for L/D=0.6. a) NB-plane. b) B-plane.

For L/D=1.2, the spectra of the pressure fluctuations exhibit a maximum in the reattachment broadband high frequencies, for x/D~0.72 in the NB-plane and for x/D~1 in the B-plane (Figure 9). The spectra obtained downstream of these reattachment points (x/D=0.99 and x/D=1.15 in the NB-plane, x/D=1.15 in the B-plane) are reminiscent of that measured in the upstream shear layer (not shown here), hence confirming that the separation is strongly dissymmetric. Near the base and within the separation, we find a peak at the Strouhal number $fL/U_\infty \sim 0.37$, still clearly identifiable in both planes, even near the reattachment points.

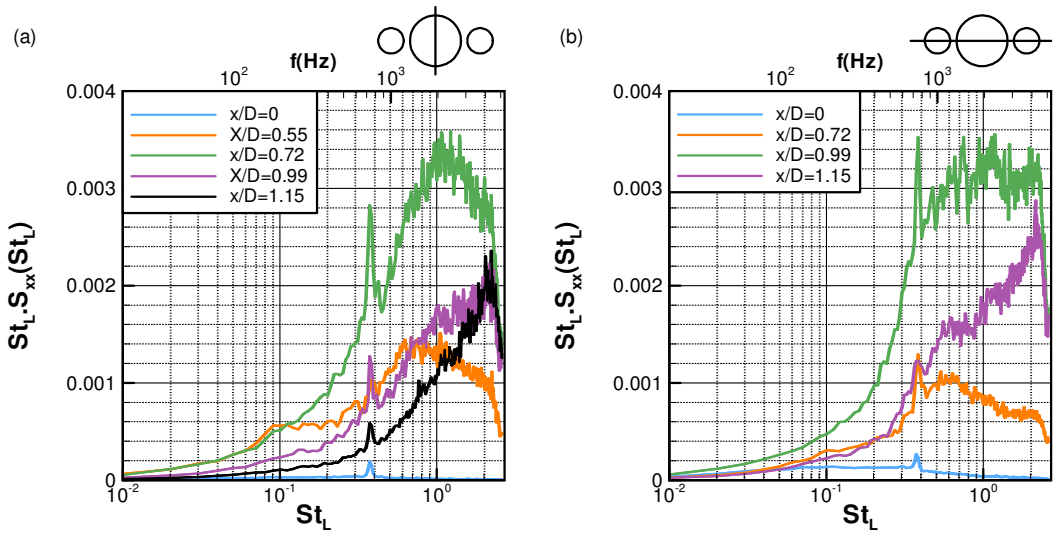

Figure 9. Spectra of the pressure fluctuations for L/D=1.2. a) NB-plane. b) B-plane.

Figure 10 presents the coherence spectra for the modes of azimuthal wavenumbers $|m| < 4$ within the separation. A comparison with Figures 3b and 4b shows that the m=0 and the m=1 modes have somehow exchanged roles: for both ratios, the m=1 undergoes a brutal loss of coherence at its peak frequency ($fD/U_\infty \sim 0.31$ for L/D=0.6 and $fL/U_\infty = 0.37$ for L/D=1.2), whereas the m=0 mode contributes for more than 90% in the fluctuations observed at this frequency.

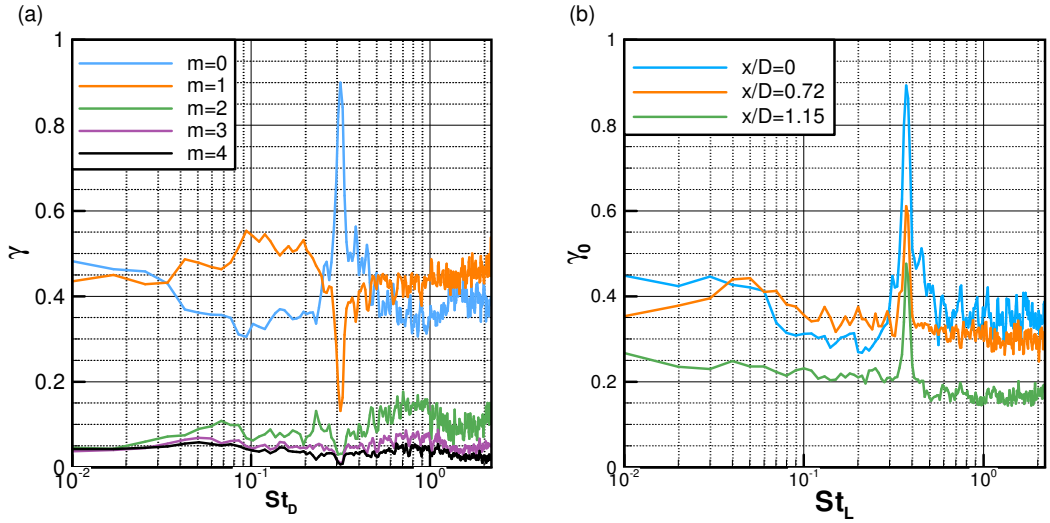

Figure 10. a) Spectra of the first five azimuthal modes at the streamwise position X/D=0.12 (L/D=0.6). b) Spectra of the m=0 mode for different streamwise positions (L/D=1.2).

An interesting point is that the peak frequency, when made non-dimensional by use of the boosters diameter is $f\Delta_b/U_\infty = 0.20$ for both values of L/D, a frequency typical of vortex shedding phenomena. Although several hypothesis are still to be considered to present a clear picture of the physical phenomena responsible for this new spatial organization, we believe that a global pressure coupling exists between the dynamics of the separated area and the wake dynamics developing downstream of the boosters. Another interesting point is that this spatial organisation of the separation strongly contrasts with that documented in other studies involving different shapes of three-dimensional afterbodies, who report frequency and azimuthal wavenumber selections identical to that documented for the axisymmetric models[1]. We believe that this difference can be ascribed to the choice of the struts

device, that may force the symmetry of the incoming flow. A wake dynamics at the vortex shedding frequency prevailing in the separated area could then be the result of a use of a dissymmetric device, although confirmation can only comes from new experimental data.

IV. Conclusion

In this study, we investigate the unsteady properties of three-dimensional afterbodies by use of wall-pressure measurements. We find that the whole flow dynamics is significantly altered by the presence of boosters. In particular, the separated area is strongly dissymmetrical with respect to the two symmetry planes of the models, with a significant increase of the fluctuations level, compared to the case of axisymmetric models. Another major effect is the presence of a narrow peak at the frequency $fl/U_\infty \sim 0.34$, associated with a highly axisymmetric mode, thus contributing weakly to the side loads.

New wind tunnel tests are also to be run to gain a more insight into the physical phenomena at work in this three-dimensional effect, in particular we aim at validating the coupling hypothesis. To this end, we plan to use three-body models equipped with supplementary sensors at the surface of the boosters to analyse the correlations between the nozzle and the boosters. We will also consider the impact of the struts on the flowfield dynamics: additional struts will be mounted parallely for each booster with a non-zero angle with respect to the B-plane, thus leading to an antisymmetric device, and the frequency and azimuthal wavenumber selection will be compared to that discussed in the present study.

Acknowledgments

The authors thank the Centre National d'Etudes Spatiales (CNES) for financial support within the framework of the research and technology program ATAC (Aérodynamique des Tuyères et Arrière-Corps). The Ph.D. dissertation of P. Meliga is funded by CNES and ONERA.

References

[1]David, C. and Radulovic, S., "Prediction on buffet loads on the Ariane 5 Afterbody", 6th International Symposium on Launcher Technologies, Munich, 2005.

[2]Délery, J. and Sirieix M., "Base flow behind missiles", AGARD LS-98 Conference, 1979.

[3]Deprés, D., "Analyse physique et modélisation des instationnarités dans les écoulements d'arrière-corps transsoniques". *Thèse de Doctorat*, ONERA - Université de la Méditerranée Aix-Marseille II (2003).

[4]Deprés, D., Radulovic, S. and Lambaré, H, "Reduction of unsteady effects in afterbody transonic flows", 6th International Symposium on Launcher Technologies, Munich, 2005.

[5]Deprés, D., Reijasse P. and Dussauge J.P., "Analysis of unsteadiness in afterbody transonic flows", *AIAA Journal* Vol. 42, 2004, pp. 2541, 2550.

[6]Eldred, K.M., "Base pressure fluctuations", *Journal of the Acoustical Society of America* Vol. 33, 1961, pp. 59,63.

[7]Flodrops, J.P. and Desse J.M., "Sillage d'un Culot Axisymétrique", *Inst. de Mécanique des Fluides de Lille*, Rept. IMFL 85L/19, 1985.

[8]Mabey, D.G., "Some measurements of base pressure fluctuations at subsonic and supersonic speeds", *Aeronautical Research Council*, ARC-CP-1204, 1972.

[9]Mabey, D.G., "Pressure fluctuations caused by separated bubble flows at subsonic speeds", Royal Aircraft Establishment, Bedford, England. RAE-TR-71160, 1971.

[10]Meliga, P., Reijasse P. and Chomaz J.M., "Effect of a serrated skirt on the buffeting phenomenon in transonic afterbody flows", IUTAM Symposium on Unsteady Separated Flows and their Control, Corfu, 2007.

[11]Merz R.A., "Subsonic base pressure fluctuations", *AIAA Journal* Vol. 17, 1979, pp 436, 438.